PHYSICAL REVIEW LETTERS

Predictive Nucleation of Crystals in Small Volumes and Its Consequences

Romain Grossier, Zoubida Hammadi, Roger Morin, and Stéphane Veesler[*]

CNRS, Aix-Marseille University, CINaM (Centre Interdisciplinaire de Nanosciences de Marseille),
Campus de Luminy, Case 913, F-13288 Marseille Cedex 09, France

We propose another way of getting to the bottom of nucleation by using finite volume systems. Here we show, using a sharp tip, that a single nucleation event is launched as soon as the tip touches the supersaturated confined metastable solution. We thus control spatial and temporal location and demonstrate that confinement allows us to carry out predictive nucleation experiments. This control is a major step forward in understanding the factors influencing the nucleation process and its underlying physics.

We still lack a comprehensive theory of crystal nucleation from solution, mainly due to the fact that experiments on nucleation are generally of a stochastic nature: we do not know where and when an indefinite number of nucleation events will occur. We thus need to observe a large number of single nucleation events when working on this phenomenon. Usually, this problem is addressed by performing a statistical analysis on a large sample of single nucleation events, for instance a statistical distribution of induction times [1]. Researchers interpret experimental data using either two-step or classical nucleation theories [2] to test both theories, but this approach is indirect. A direct method would consist in exploring the crystal precursor, that is, the critical nucleus. Unfortunately, there are few reports of observation of critical nuclei in bulk materials [3–6] because critical clusters are rare and randomly distributed. We propose another way of getting to the bottom of nucleation, here applied to crystallization in solution, by using confined systems, i.e., finite volume systems whose volume affects nucleation. Here we show, using a sharp tip, that a single nucleation event is launched as soon as the tip touches the supersaturated confined metastable solution. We thus control spatial and temporal location and demonstrate that confinement allows us to carry out predictive nucleation experiments. This control is a major step forward in understanding the factors influencing the nucleation process and its underlying physics. A better understanding of nucleation will open the way to new approaches to crystallization in production, for instance of pharmaceuticals and nanomaterials, as well as in biomineralization studies, for instance on the formation of bones, teeth, and shells.

Emulsion-based methods such as microfluidics [7,8], are appropriate to study nucleation because it is statistically better to have hundreds of independent small-volume nucleation experiments (typically in the nanoliter range) instead of one larger volume experiment (typically in the microliter to milliliter range). Nucleation frequency depends on volume: the smaller the volume, the longer the induction time, which increases the supersaturation range

to be experimentally accessible [9]. However, we have recently demonstrated, using a simple thermodynamics model relying only on the existence of a critical size and the evolution during nucleation and growth process of the supersaturation in a confined system (a small droplet), that there is another, unforeseen, influence of volume on nucleation from the picoliter range to a smaller range [10], in agreement with experimental results showing the effects under nanoscopic confinement [11–15]. In these small-volume systems, unexpected high-supersaturated metastable solutions are observed due to this confinement effect. In other words, below a critical initial supersaturation, no nucleation can occur. This is because the depletion of the solution decreases the supersaturation, thus increasing the critical size that needs to be reached. In essence, however much the precritical cluster chases the critical size, it can never catch it [10].

In the experiments presented in this Letter, supersaturation is generated via the droplet contraction technique [16]. Aqueous phase microdroplets of controlled size, ranging from nanoliter to femtoliter, are generated in oil by a fluidic device developed in our group (Fig. 1) [18]. Experiments are performed under an optical microscope (Zeiss Axio
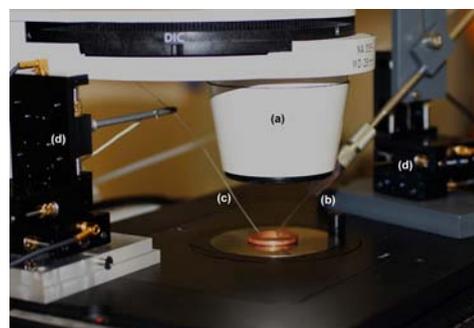

FIG. 1 (color online). Image of the whole experimental setup, (a) microscope, (b) glass capillary, (c) tungsten wire sharp tip, Supplemental Material [17] contains transmission electron micrographs of tungsten tips, and (d) *XYZ* miniature translation stages.

Observer D1), on an 18 mm-diameter glass coverslip treated in such a way as to obtain a hydrophobic surface (4%-950 K PMMA) to avoid microdroplet spreading and coalescence. The coverslip can be thermostatted and is covered with approximately 100 μL of inert dodecamethylpentasiloxane (DMS) oil (Hampton Research HR3-593, refractive index = 1.390). The micrometer-sized droplets of aqueous phase solution are generated on the coverslip by a microinjector (Femtojet, Eppendorf). Two homemade micromanipulators consisting of three miniature translation stages (piezoelectric elements, MS30 Mechonics) allow the injector (capillary holder) and the tip (tungsten wire) to be moved in X, Y, and Z with a displacement range of 18 mm in the three directions by steps of 16 nm. We use a glass capillary (the micropipette) with an internal diameter of 0.5 μm (Femtotip Eppendorf) and a homemade sharp tip produced by electrolytic etching [19,20] of a 125 μm tungsten wire. The whole setup is shown in Fig. 1. Chemical compositions for the different experiments are specified in the figures.

The diffusion of the solvent, water, into the oil drives the creation of high supersaturation. As pointed out above, we expect greater metastability for finite-sized systems (small-volume systems). The NaCl concentration is qualitatively monitored through the evolution of the optical contrast between the droplet and the continuous phase (the oil). At $t = 0$, the refractive index of the 4.5 M NaCl solution is 1.373 and when the solution concentrates during diffusion of water the refractive index increases. Here it was vital to identify a medium matching the refractive index of the droplet at the time of nucleation. After extensive experiments, we identify n-dodecane (refractive index = 1.422) as the most suitable continuous phase, as supported by the fact that nucleation occurs when microdroplets disappear. NaCl concentration is thus estimated from a relation between concentration and refractive index (Tables 71 D-252) [21]. Using this estimation, we calculate the supersaturation in the droplets at the nucleation time to be $\beta > 1.97$. Supersaturation ß is defined as the ratio of the NaCl concentration in solution versus the solubility concentration of NaCl, 5.42 M at 20 °C in water [22]. Note that nonconfined NaCl solutions spontaneously nucleate at $\beta > 1.03$.

Once supersaturation is established, the usual approach is to wait for nucleation events, which cannot be precisely predicted in space and time, to occur. The time of observation of detectable crystals therefore cannot be equated with the induction time, because the growth rate is not known. In our approach, we know where nucleation will occur—in the microdroplets (Fig. 2)—and we have a fast growth rate due to confinement ($\approx 10 \mu$m/s) [15]. Because of the fast growth rate, the time required for the newly formed nuclei to grow to a detectable size is negligible with regard to the induction time. Thus, the time when a detectable crystal is observed is really the induction time. However, even though we realize spatial control of nucleation via confinement in the microdroplet,
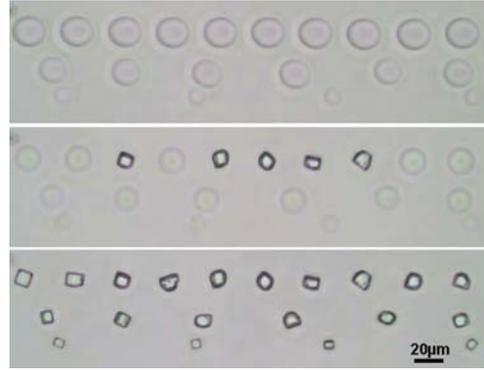

FIG. 2 (color online). Time sequence showing nucleation and fast growth of NaCl crystals. (a) At $t = 0$ 4.5 M NaCl microdroplets of volumes ranging from 3 to 1 pL are generated (assuming a spherical shape for the droplet), (b) $t = 4638$ s, and (c) $t = 6120$ s. All the micrographs are at the same magnification.

experimental results summarized in Table I clearly illustrate that nucleation is still stochastic. Complete statistical analysis of induction time distribution [1,24] obtained with this setup is beyond the scope of this Letter, but is in progress in our group.

Here we focus on spatial and temporal control of nucleation and its consequences. We use a sharp tip to induce a single nucleation event by touching the supersaturated metastable microdroplet of KCl solution [Figs. 3(a) and 3(b)]. The period when the microdroplet can be touched is either determined from the above experiments, like that presented in Fig. 2 (where the period is between the time when supersaturation is established and the induction time, see Table I), or can be estimated by a trial and error method: the droplet is repeatedly tapped

TABLE I.   Induction times in the different microdroplets from experiment of Fig. 2.

Induction time[a] (s)		
Volume: 3 pL	Volume: 2 pL	Volume: 1 pL
2107	4252	4450
2595	4335	4552
2856	4338	4570
3064	4363	4828
3301	4501	
3787	4711	
4152		
4197		
4458		

[a]Induction time t is the difference between the time of appearance of a crystal in the microdroplet and the time when supersaturation is established, that is to say when water diffusion from microdroplet into oil is stopped. When the solute concentration increases, the vapor pressure of the mixture decreases. This effect stops evaporation, giving rise to a highly supersaturated droplet, as observed by Tang *et al.* [23]. Induction time is estimated optically from the variation of the refractive index, here $t = 1269$ s.
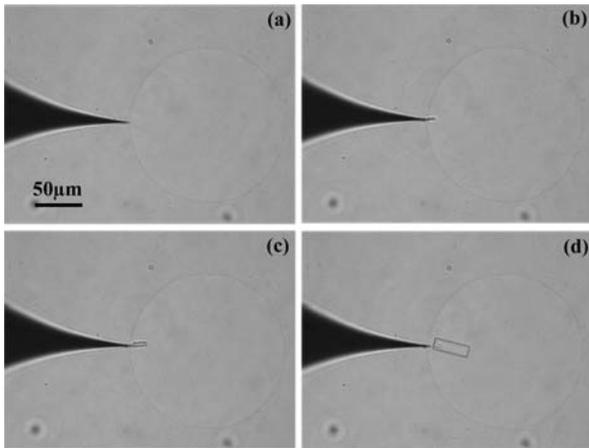
FIG. 3. Panels (a)–(d) represent a time sequence showing the nucleation and growth of KCl in DMS oil, initial condition: undersaturated KCl solution ($\beta = 0.5$), (a) droplet size 147 μm (≈ 1.66 nL assuming a spherical shape for the droplet). All the micrographs are at the same magnification, the time between (b) and (d) is 1.3 s.

with the sharp tip during the generation of supersaturation by water diffusion. In both cases, once the threshold level of supersaturation is reached, tapping launches nucleation instantaneously (Fig. 3). The time between tip contact and observation of nucleation is shorter than 0.1 s (at the resolution of our image acquisition system, 10 Hz).

Note that we also succeeded in controlling nucleation with a wide variety of aqueous phases, namely KNO_3, $CaSO_4 \cdot 2H_2O$, NaCl, glycine, and bovine pancreatic trypsin inhibitor.

We used a different tip approach, increasing tip penetration, with droplets of NaCl solutions. This too launched instantaneous nucleation, but here the crystal remains attached to the tip during growth [Figs. 4(a)–4(d)]. This enables the single crystal to be moved and handled as shown in Figs. 4(e) and 4(g)–4(l). First, the crystal is withdrawn from the microdroplet and moved to seed another supersaturated metastable microdroplet [Figs. 4(e)–4(g)], and then left to grow [Figs. 4(g)–4(i)]. Second, the crystal and the microdroplet are fused with another supersaturated metastable microdroplet [Fig. 4(i)]. Note that in our experiment, during this operation a second crystal nucleated [indicated by an arrow in Fig. 4(k)]. Finally, the crystal is withdrawn from the microdroplet [Fig. 4(l)]. This ability to handle the crystal holds great promise for numerous applications.

This Letter shows how we achieve spatial and temporal control of nucleation, yielding the first direct method for studying nucleation. We conduct our nucleation experiments in two steps: first, we stabilize unusually high supersaturated solutions and, second, we induce a structural transformation via mechanical contact at precisely determined points. This is in line with the two-step nucleation theory and with recent experimental results obtained on protein crystallization [25,26] showing that when
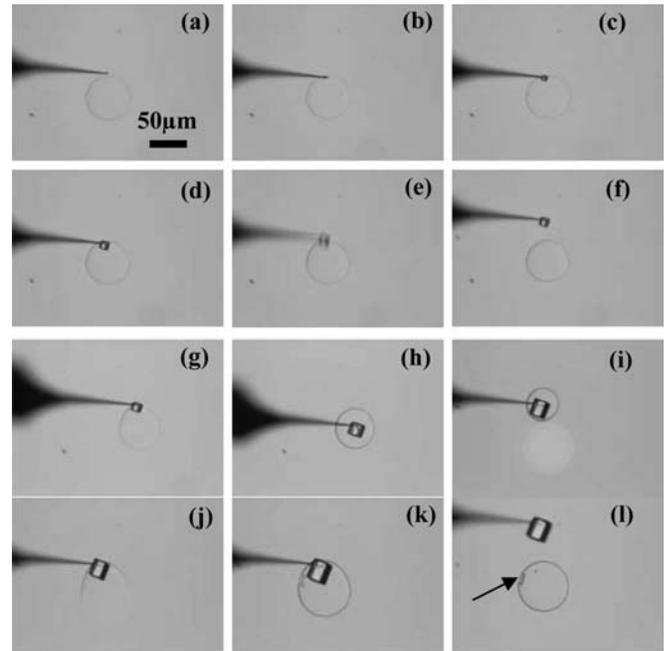

FIG. 4. Panels (a)–(l) represent a time sequence showing the nucleation and growth of NaCl at supersaturation $\beta > 1.97$. (a) 0.7 M NaCl initial droplet size 56 μm (≈ 51 pL assuming a spherical shape for the droplet). All the micrographs are at the same magnification. See Supplemental Material [17] for a movie of this process.

liquid-liquid phase separation occurs, microdroplets of protein-rich phases (high concentrated solutions) are stable [25,27] with respect to nucleation. Moreover, any disturbance, for instance a crystal touching the dense droplets [26], triggers nucleation.

Because of the deterministic nature of the nucleation experiments presented in this Letter, investigation of the critical cluster is now possible. We already have the tools to observe such small groups of molecules and now we know where and when the critical cluster will appear.

*veesler@cinam.univ-mrs.fr

[1] D. Knezic, J. Zaccaro, and A. S. Myerson, J. Phys. Chem. B **108**, 10672 (2004).

[2] D. Kashchiev, *Nucleation: Basic Theory with Applications* (Butterworth-Heinemann, Oxford, 2000), p. 529.

[3] S. T. Yau and P. G. Vekilov, Nature (London) **406**, 494 (2000).

[4] U. Gasser *et al.*, Science **292**, 258 (2001).

[5] K.-Q. Zhang and X. Y. Liu, Nature (London) **429**, 739 (2004).

[6] K. F. Kelton *et al.*, Phys. Rev. Lett. **90**, 195504 (2003).

[7] P. Laval, A. Crombez, and J.-B. Salmon, Langmuir **25**, 1836 (2009).

[8] J.-U. Shim et al., Cryst. Growth Des. **7**, 2192 (2007).

[9] M. Ildefonso, N. Candoni, and S. Veesler, Cryst. Growth Des. **11**, 1527 (2011).

[10] R. Grossier and S. Veesler, Cryst. Growth Des. **9**, 1917 (2009).

[11] J.-M. Ha et al., J. Am. Chem. Soc. **126**, 3382 (2004).

[12] M. Beiner et al., Nano Lett. **7**, 1381 (2007).

[13] K. Kim et al., J. Am. Chem. Soc. **131**, 18212 (2009).

[14] C. J. Stephens et al., Adv. Funct. Mater. **20**, 2108 (2010).

[15] R. Grossier, A. Magnaldo, and S. Veesler, J. Cryst. Growth **312**, 487 (2010).

[16] O. A. Bempah and O. E. Hileman, Jr., Can. J. Chem. **51**, 3435 (1973).

[17] See Supplemental Material at http://link.aps.org/supplemental/10.1103/PhysRevLett.107.025504 for transmission electron micrographs of tungsten tips and a movie of the tip-tapping nucleation process.

[18] R. Grossier et al., Appl. Phys. Lett. **98**, 091916 (2011).

[19] E. W. Muller and T. T. Tsong, Field Ion Microscopy: Principles and Applications (American Elsevier Publishing Company, New York, 1969).

[20] Z. Hammadi, M. Gauch, and R. Morin, J. Vac. Sci. Technol. B **17**, 1390 (1999).

[21] Handbook of Chemistry and Physics (CRC Press, Cleveland, 1975).

[22] H. Langer and H. Offermann, J. Cryst. Growth **60**, 389 (1982).

[23] I. N. Tang and H. R. Munkelwitz, J. Colloid Interface Sci. **98**, 430 (1984).

[24] L. Goh et al., Cryst. Growth Des. **10**, 2515 (2010).

[25] S. Grouazel et al., J. Phys. Chem. B **110**, 19664 (2006).

[26] D. Vivares, E. W. Kalera, and A. M. Lenhoff, Acta Crystallogr. Sect. D **61**, 819 (2005).

[27] R. M. L. Evans, W. C. K. Poon, and M. E. Cates, Europhys. Lett. **38**, 595 (1997).